Techno-Economic Evaluation of the Retrofitted Power-to-Methanol Process: Grid-connected Energy Arbitrage vs Standalone Renewable Energy

Siphesihle Mbatha[a,b,*], Payam G. Panah[c], Xiaoti Cui[c], Paulo Debiagi[d], Benoit Louis[e], Nicholas M. Musyoka[d,**], Raymond C. Everson[b], Ksenia Parkhomenko[e], Henrietta W. Langmi[f]

[a] *HySA Infrastructure Centre of Competence, Centre for Nanostructures and Advanced Materials (CeNAM), Chemicals Cluster, Council for Scientific and Industrial Research (CSIR), Pretoria 0001, South Africa*

[b] *Centre of Excellence in Carbon Based Fuels, School of Chemical and Minerals Engineering, Faculty of Engineering, North-West University, Private Bag X6001, Potchefstroom, 2531, South Africa*

[c] *Department of Energy, Aalborg University, Pontoppidanstr. 111, 9220 Aalborg, Denmark*

[d] *Nottingham Ningbo China Beacons of Excellence Research and Innovation Institute, University of Nottingham Ningbo China, Ningbo 315100, PR China*

[e] *Institute of Chemistry and Processes for Energy, Environment and Health (ICPEES), UMR 7515 CNRS-University of Strasbourg, 25 rue Becquerel, Strasbourg 67087 Cedex 02, France*

[f] *Department of Chemistry, University of Pretoria, Private Bag X20, Hatfield, 0028, South Africa*

*Correspondence Emails: siphe.mbatha94@gmail.com, **Nicholas.Musyoka@nottingham.edu.cn

ABSTRACT

The geopolitical and climate imperatives to diversify energy supply and transition to cleaner energy and fuel alternatives continue to gain momentum in the global sphere. In this regard, power-to-methanol (PtMeOH) will play a crucial role as a form of renewable chemical energy storage, and it promises more than its alternatives. In this paper, the PtMeOH process techno-economics is assessed using the promising configuration described in our previous work (Mbatha et al. [1]). This study squarely focuses on the evaluation of the effect of the parameters such as the CO_2 emission tax, electricity price, and the CAPEX reduction to realise of the product methanol economic parity. A scenario where existing methanol synthesis infrastructure is 100% retrofitted with the promising electrolyser is investigated in terms of its economics and the associated economic parity. The South African market volatility in the electricity price and its impact on the process's economic viability is considered. Under this caveat, the sensitivity of the PtMeOH vs green H_2 profitability is checked considering aforementioned parameters. The grid connected and the standalone renewable energy scenarios are assessed. Generalisable effect trends of these parameters on the NPV and the levelized cost of methanol and H_2 are discussed. The results show that economic parity of H_2 (LCOH2 = current selling price = 4.06 €/kg) can be reached with an electricity price of 30 €/MWh and 70% of the CAPEX. While the LCOMEOH will still be above 2 €/kg at 80% of the CAPEX and electricity price of 20 €/MWh. This indicates that even if the CAPEX reduces to 20% of its original in this study, and the electricity price reduces to about 20 €/MWh, the LCOMEOH will still not reach economic parity (LCOMEOH > current selling price = 0.44 €/kg). The results show that to make the retrofitted plant profitable, a feasible reduction in the electricity price to below 10 €/MWh along with favourable incentives such as CO_2 credit and reduction in CAPEX, particularly the electrolyser, and treatment of the PtMeOH as a multiproduct plant will be required.

Key words: *Power-to-Methanol, Green Hydrogen, Solid oxide electrolyser, Techno-Economics, Sensitivity Analysis, Grid-connected, Standalone Renewable Energy.*

Section S1: Electrolysis

Both AWE and PEM are well-established and commercialized; hence, investment in such projects is more attractive [2], [3-4]. SOEC can also be profitable with promoted hydrogen and low-price electricity[2]. With the several advantages of SOEC, such as its bidirectional operation and higher efficiency, several studies have shown the promising potential of SOEC as a candidate electrolysis technology of the future [15] as discussed in the literature survey of the paper. Figure S1 shows the heat integrated SOEC flowsheet model in Aspen Plus.

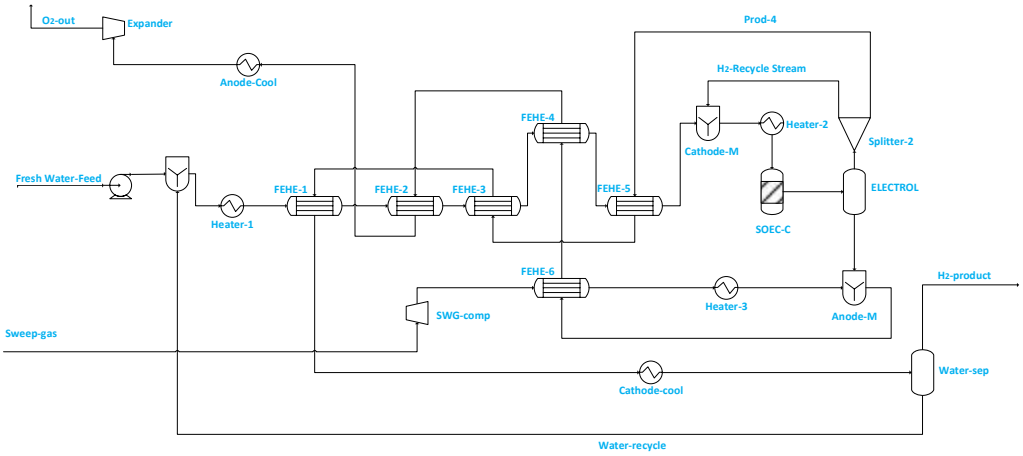

Figure S1 Illustration of the SOEC unit used for steam electrolysis in ASPEN PLUS®.

Section S2: Methanol Reactor and Separator system modelling

The reactor size was selected to be large enough such that the effluent from the reactor is near equilibrium [9]. Figure S2 show the process flow diagram for the methanol synthesis unit modelled in this work. Redlich-Kwong-Soave equation of state with modified Huron-Vidal mixing rules (RKSMHV2) was used to model the reactor(s), auxiliaries and to calculate the thermodynamic properties of the streams. After separation of methanol and water using a flash drum, a recycle stream was then purged up to 0.1% for all flowsheets. In line with the work of Cui *et al*., the small purge of 0.1% was set, which aims to minimize the CO_2 emission for the green methanol production [10]. As observed from Cui et al. using a larger purge ratio can result in lower flow rate of the recycle stream as well as a smaller reactor size but a higher CO_2 loss. It was also observed from Cui et al. that a value lower than 0.1% may cause convergence problem [10]. For the syngas (co-electrolysis-based system), the purge stream after methanol separation and recycle was set to 1.3%. The reactor considered in this study is the adiabatic reactor. The advantage of adiabatic fixed bed methanol synthesis reactor is that under nominal steady state conditions their size is very small, thus their over-sizing slightly affect the capital cost [5-7]. This indicates their potential in small scale PtMeOH processes as well [8].

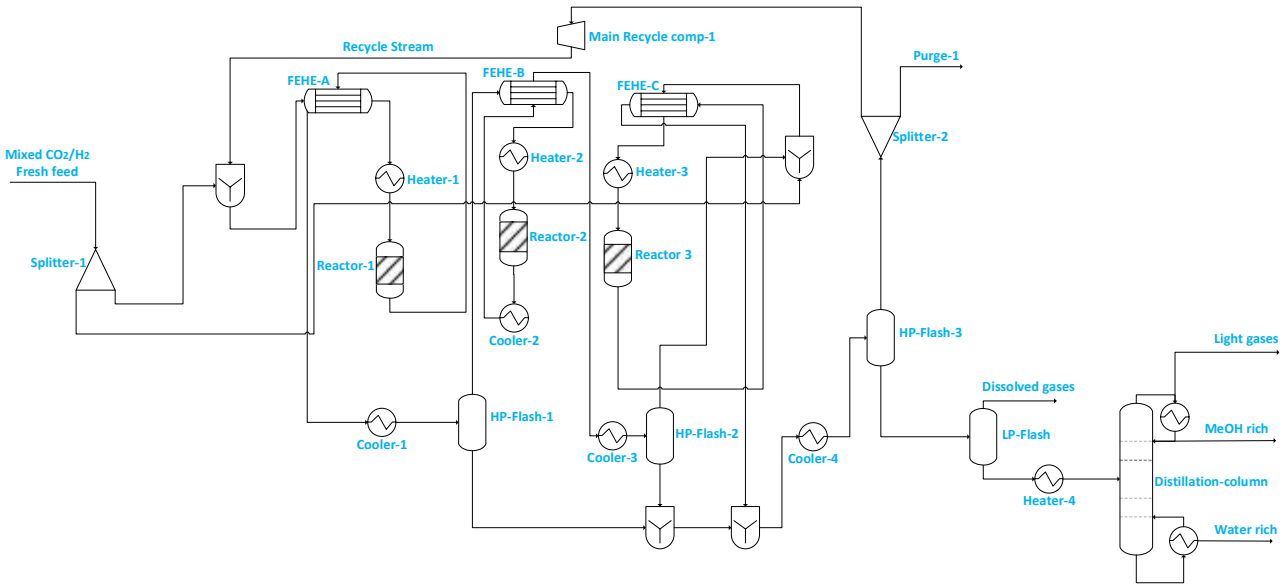

Figure S2 Illustration of the methanol synthesis unit used for steam electrolysis in ASPEN PLUS®.

Table S1: Adiabatic plug-flow reactor (s) operating conditions

Parameter	Value	Unit
Reactors volume	24-35	m^3
Reactor inlet pressure	75.7	bar
Catalyst particle density	1775	kg/m^3
Bed porosity	0.5	-
GHSV	4000-7300	h^{-1}

2.1. Reaction kinetics

Industrially, methanol is synthesized from syngas following the three main equilibrium reactions as expressed by Eq. 1-3 over an industrial $Cu/ZnO/Al_2O_3$ catalyst. However, it is has been recently agreed and demonstrated that methanol can also be produced from a feed with pure CO_2/H_2 i.e., via Eq. 3 only even though the actual reaction mechanism and carbon source for methanol remains an active subject of debate [11-14].

$$CO_2 + 3H_2 \leftrightarrow CH_3OH + H_2O \qquad \Delta H_{298K} = -49.43 kJ/mol \qquad (1)$$

$$CO_2 + H_2 \leftrightarrow CO + H_2O \qquad \Delta H_{298K} = +41.12\ kJ/mol \qquad (2)$$

$$CO + 2H_2 \leftrightarrow CH_3OH \qquad \Delta H_{298K} = -90.55\ kJ/mol \qquad (3)$$

Following Le'Chaterliers principle, higher methanol yields are favoured at lower temperatures and higher pressures. However, for the reason of enhancing kinetics, temperatures in the range of temperature 200–300 °C are used as well as high pressure ranges of 50-100 bar over the commercial $Cu/ZnO/Al_2O_3$ catalyst. The reverse water gas shift reaction (Eq. 3) is the only endothermic reaction in the three main reactions and therefore gets promoted as temperature increases. This reaction increases the amount of water generated in the case when pure CO_2/H_2 is the main feed. This lowers the selectivity to methanol and the catalyst activity. As a result, significant research efforts are devoted to

the CO_2 hydrogenation to methanol process, mostly to improve the catalyst conversion and selectivity [15-16]. However, the commercial $Cu/ZnO/Al_2O_3$-based catalyst is likely to remain the best possible for some time due to its ability to achieve highest yield, its low costs, and high stability [16]. Ruland et al. established, through dynamic experimental conditions relevant to power-to-methanol (PtMeOH), that the industrial $Cu/ZnO/Al_2O_3$ is highly stable for conditions of chemical energy storage with hydrogen produced from fluctuating renewable energy sources, indicating its relevance for application in PtMeOH [17]. Besides the challenges of optimizing the catalyst beyond what the commercially available catalyst can achieve to promote CO_2/H_2 to methanol, this reaction is attractive from an environmental perspective in that a significant quantity of CO_2 can be recycled, and in addition it is less exothermic, thus rendering ease of heat management in the reactor, and fewer by-products formation. For these reasons and following the most recent kinetic analysis such as in the work of Nestler et al, Slotboom et al., and de Oliveira Campos et al., who deduced that the role of CO hydrogenation to methanol is negligible at high CO_2/CO feed ratio, in this work and only reactions 3 and 4 are considered in the modelling of the methanol synthesis [18-20].

The kinetic model used in this study was presented in the work of Van-Dal & Bouallou [6], which originated initially from the model of Bussche and Froment [5],[7]. The model assumes methanol production from CO_2 hydrogenation (i.e., Eq. 1) in the presence of RWGS as a competing reaction (Eq. 3) and absence of diffusional limitations. Thus, the effectiveness factor equals 1 [21]. The kinetic model is based on Langmuir Hinshelwood Hougen-Watson (LHHW) kinetic model formulation and is expressed by Eq. 4 and 5.

$$r_{CH_3OH} = \frac{k_1 P_{CO_2} P_{H_2} - k_6 P_{H_2O} P_{CH_3OH} P_{H_2}^{-2}}{\left(1 + k_2 P_{H_2O} P_{H_2}^{-1} + k_3 P_{H_2}^{0.5} + k_4 P_{H_2O}\right)^3} \quad \left[\frac{kmol}{kg_{cat}s}\right] \tag{4}$$

$$r_{RWGS} = \frac{k_5 P_{CO_2} - k_7 P_{H_2O} P_{CO} P_{H_2}^{-1}}{1 + k_2 P_{H_2O} P_{H_2}^{-1} + k_3 P_{H_2}^{0.5} + k_4 P_{H_2O}} \quad \left[\frac{kmol}{kg_{cat}s}\right] \tag{5}$$

Where k_i were calculated for implementation in ASPEN PLUS V11® using the Eq. 6 and these are tabulated in Table S2 below.

$$\ln k_i = A_i + \frac{B_i}{T} \tag{6}$$

Table S3 presents the main parameters of the distillation column which was modelled as RadFrac in ASPEN PLUS V11®. NRTL-RK was selected as a property method to model the distillation column and its feed (with pressure ≤1.1bar).

Table S2: Kinetic parameters rearranged for implementation in ASPEN PLUS V11® as a LHHW model [5-7].

Kinetic parameters	Ai	Bi
k_1	-29.87	4811.2
k_2	8.147	0
k_3	-6.452	2068.4
k_4	-34.95	14928.9
k_5	4.804	-11797.5
k_6	17.55	-2249.8
k_7	0.1310	-7023.5

Table S3: Main parameters of the distillation column used for final separation of methanol.

Parameter	Value	Unit/basis
Column	RadFrac	-
Number of trays	30	-
Condenser type	Partial-Vapor-Liquid	-
Reflux ratio	1.5	mole
Boilup ratio	1.2	mole
Feeding temperature	80	°C
Operating pressure	1.1	bar

Validation of the kinetic model is presented in the supplementary material section S3. The typical catalyst pellets of 6mm×4mm was packed in the catalyst bed and Ergun equation was used for pressure drop calculation through the catalyst bed. Following process engineering principles, the reactors were sized at constant total reactor(s) volume. A hold-up time of 5 minutes was used in sizing the separators, and the compressor curves were used to model the compressors. The methanol reactor model developed by using Aspen Plus was validated by comparing with the simulation results in Van den Bussche and Froment [5]. Good agreement was shown in Fig. S3. The operating conditions for the simulation of the methanol reactor were also given in Van den Bussche and Froment [5].

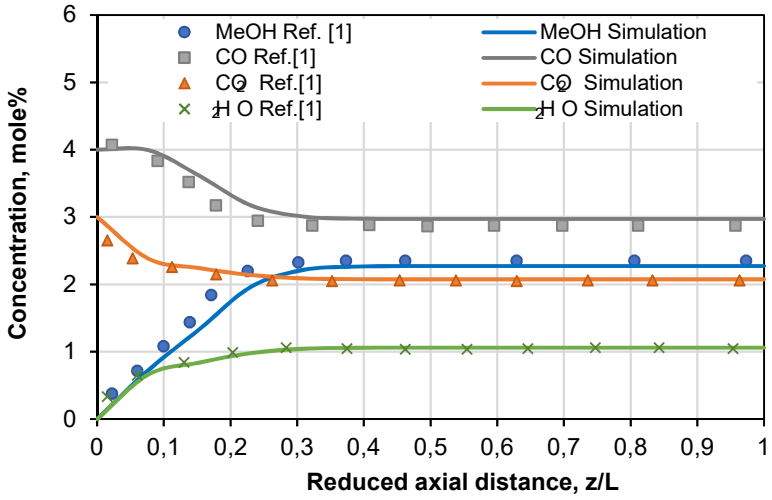

Figure S3. Model predicted vs experimental gas composition.

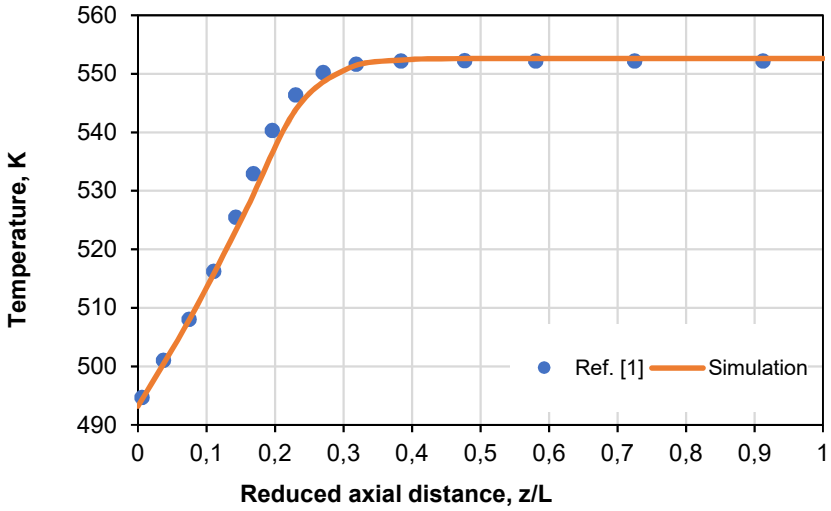

Figure S3. Temperature profiles along the methanol reactor under the operation conditions in Van den Bussche and Froment [5].

Ergun equation

The pressure drop over the catalyst bed was evaluated by the following Ergun equation (4):

$$\frac{dP}{dz} = -(1.75 + 150\frac{1-\varepsilon}{Re_p^s})\frac{1-\varepsilon}{\varepsilon^3}\frac{\rho_f u^2}{d_p^s} \quad (6)$$

Section S3: Detailed Mass and Energy Balance of the Unit

Table S4: Mass and Energy balance of critical equipment (see MEOH synthesis flowsheet in Figure 2 below)-including BOP for SOEC (Fig 1 below)

								Current plant design	
Component	**Mass flow in**	**Units**	**Number of equipment**	**Energy Consumption**	**Units**	**Size**	**Units**	**Equipment Cost ($)**	**Total Installed Fixed cost ($)**
Pump	22101.5	kg/h	1	5.8	kW	8.15	l/s	9257.0	16051.7
Compressor 1	17650	kg/h	1	478.3	kW	478.3	kW	2209793.0	3831781.1
Compressor 2	17650	kg/h	1	537.3	kW	537.3	kW	2319351.2	4021755.0
Compressor 3	17650	kg/h	1	486.9	kW	486.9	kW	2226193.8	3860220.0
Compressor 4	17650	kg/h	1	448.7	kW	448.7	kW	2151782.1	3731190.1
Compressor 5	2702.4	kg/h	1	2620.0	kW	2620.0	kW	4485416.0	7777711.3
Compressor 6	2702.4	kg/h	1	1638.2	kW	1638.2	kW	3688979.5	6396690.4
Compressor 7	1000.0	kg/h	1	58.4	kW	58.4	kW	920632.4	1596376.6
Compressor 8	11997.7	kg/h	1	232.8	kW	232.8	kW	1637418.4	2839283.4
Expander	20399.3	kg/h	1	-550.8	kW	-550.8	kW	84172.7	145955.5
Reactor 1	31943.3	kg/h	1	-	-	34.3	m3	293253834.5	508502149.1
Reactor 2	22013.9	kg/h	1	-	-	26.9	m3	266677453.8	462418704.9
Reactor 3	15888.8	kg/h	1	-	-	23.9	m3	248145153.3	430283695.8
Distillation column (empty)	20232.5	kg/h	1	7000.0	kW	338.7	tons/d	42268374.0	73293360.5

								Current plant design	
Component	**Mass flow in**	**Units**	**Number of equipment**	**Energy Consumption**	**Units**	**Size**	**Units**	**Equipment Cost ($)**	**Total Installed Fixed cost ($)**
Distillation column Trays (Sieve)	20232.5	kg/h	10 trays *3	7000.0	kW	2.3	m	93397.1	161950.5
Flash drum 1	10180.4	kg/h	1	-7.86E-12	kW	526.1	m3	140609.1	243816.2
Flash drum 2	31943.3	kg/h	1	0.37	kW	125.5	m3	62109.7	107698.2
Flash drum 3	22014.3	kg/h	1	-2.1E-12	kW	111.7	m3	58129.4	100796.3
Flash drum 4	32350.6	kg/h	1	-557.6	kW	116.6	m3	59568.4	103291.6
Flash drum 5	20340.8	kg/h	1	-621.81	kW	11.5	m3	15901.0	27572.3
Heater 1	29579.5	kg/h	1	22316.8	kW	22316.8	kW	3573399.3	6196274.4
Heater 2	31171.1	kg/h	1	2929.5	kW	2929.5	kW	1416249.0	2455775.8
Heater 3	1000.0	kg/h	1	60.7	kW	60.7	kW	241967.4	419571.4

Component	**Mass flow in**	**Units**	**Number of equipment**	**Energy Consumption**	**Units**	**Size**	**Units**	**Equipment Cost ($)**	**Total installed Fixed cost ($)**
Heater 4 (React start-up)	31943.1	kg/h	1	0 (during operation)	kW	0	kW	330306.5	572751.4
Heater 5 (React start-up)	22013.9	kg/h	1	4.49E-12 (during operation)	kW	4.49E-12	kW	330306.5	572751.4
Heater 6 (react-startup)	15888.8	kg/h	1	0(during operation)	kW	0	kW	330306.5	572751.4
Heater 7	20232.5	kg/h	1	5530.2	kW	5530.2	kW	1891986.9	3280705.3
Cooler 1	17650	kg/h	1	-407.1	kW	-407.1	kW	139888.5	242566.6
Cooler 2	17650	kg/h	1	-537.2	kW	-537.2	kW	111345.0	193072.3
Cooler 3	17650	kg/h	1	-547.2	kW	-547.2	kW	113787.9	197308.3
Cooler 4	20399.3	kg/h	1	-2667.4	kW	-2667.4	kW	166889.0	289385.5
Cooler 5	10180.4	kg/h	1	-9320.0	kW	-9320.0	kW	304463.1	527939.0
Cooler 6	2702.39	kg/h	1	-2458.4	kW	-2458.4	kW	152874.4	265084.2
Cooler 7	31943.3	kg/h	1	-9373.8	kW	-9373.8	kW	421851.1	731489.8
Cooler 8	22014.3	kg/h	1	-4789.7	kW	-4789.7	kW	387650.4	672185.9
Cooler 9	32350.6	kg/h	1	-1990.5	kW	-1990.5	kW	155703.0	269989.1
Cooler 10	642.0	kmole/h	1	-11427.1	kW	-11427.1	kW	264862.3	459271.3
FEHE 1	29579.5	kg/h	1	2501.4	kW	17.1	m2	45307.1	78562.4
FEHE 2	29579.5	kg/h	1	141.4	kW	0.6	m2	9759.7	16923.4
FEHE 3	29579.5	kg/h	1	2845.7	kW	17.8	m2	46160.0	80041.5
FEHE 4	29579.5	kg/h	1	1314.0	kW	8.9	m2	33504.2	58096.3
FEHE 5	29579.4	kg/h	1	2180.5	kW	18.3	m2	46744.5	81055.0
FEHE 6	1000.0	kg/h	1	115.7	kW	0.4	m2	7820.8	13561.3
FEHE 7	31943.1	kg/h	1	5453.8	kW	117.4	m2	110293.9	191249.5
FEHE 8	22014.3	kg/h	1	7000.3	kW	132.1	m2	116469.8	201958.6
FEHE 9	15888.9	kg/h	1	6079.1	kW	119.0	m2	110994.1	192463.7
Hydrogen storage tank	TBC	TBC	TBC	TBC	TBC	TBC	kgH2	330 [1]	US$/kgH2

Cooling water	-43518.5	kW		-43518.5	kW	-0.04	GJ	0.21	$/GJ
Unit capex of CO2 storage	TBC	TBC	TBC	TBC	TBC	TBC	TBC	3450	€/t
DC reboiler	620.9	kg/h	1	7000.0	kW	7000.0	kW	188746.6	327286.5
DC reflux pump	640.1	kmole/h	1	11.1	kWh	11.1	kWh	55286.8	95867.30619
DC-drum overhead	400.8	kmole/h	1	-	-	-		131145.4	227406.1682

Table S5: Mass and Energy balance of critical equipment (see mostly MEOH synthesis flowsheet in figure 2 below)-excluding BOP for SOEC {Note: table considered the methanol synthesis section only and the removed components can also be removed on utility table to consider only MEOH section utility}

Component	Mass flow in	Unit	Number of equipment	Energy Consumption	Unit	Size	Unit	Equipment Cost ($)	Total installed fixed cost ($)
Compressor 1	17650	kg/h	1	478.3	kW	478.3	kW	2209793.0	3831781.1
Compressor 2	17650	kg/h	1	537.3	kW	537.3	kW	2319351.2	4021755.0
Compressor 3	17650	kg/h	1	486.9	kW	486.9	kW	2226193.8	3860220.0
Compressor 4	17650	kg/h	1	448.7	kW	448.7	kW	2151782.1	3731190.1
Compressor 5	2702.4	kg/h	1	2620.0	kW	2620.0	kW	4485416.0	7777711.3
Compressor 6	2702.4	kg/h	1	1638.2	kW	1638.2	kW	3688979.5	6396690.4
Compressor 8	11997.7	kg/h	1	232.8	kW	232.8	kW	1637418.4	2839283.4
Reactor 1	31943.3	kg/h	1	-	-	34.3	m3	293253834.5	508502149.1
Reactor 2	22013.9	kg/h	1	-	-	26.9	m3	266677453.8	462418704.9
Reactor 3	15888.8	kg/h	1	-	-	23.9	m3	248145153.3	430283695.8
Distillation column (empty)	20232.5	kg/h	1	7000.0	kW	338.7	tons/d	42268374.0	73293360.5
Distillation column Trays (Sieve)	20232.5	kg/h	10 trays *3	7000.0	kW	2.3	m	93397.1	161950.5
Flash drum 1	10180.4	kg/h	1	0.0	kW	526.1	m3	140609.1	243816.2
Flash drum 2	31943.3	kg/h	1	0.4	kW	125.5	m3	62109.7	107698.2
Flash drum 3	22014.3	kg/h	1	0.0	kW	111.7	m3	58129.4	100796.3
Flash drum 4	32350.6	kg/h	1	-557.6	kW	116.6	m3	59568.4	103291.6
Flash drum 5	20340.8	kg/h	1	-621.8	kW	11.5	m3	15901.0	27572.3
Heater 4 (React 1 start-up)	31943.1	kg/h	1	0.0	kW	0.0	kW	330306.5	572751.4
Heater 5 (React 2-start-up)	22013.9	kg/h	1	0.0	kW	0.0	kW	330306.5	572751.4
Heater 6 (react 3-startup)	15888.8	kg/h	1	0.0	kW	0.0	kW	330306.5	572751.4
Heater 7 (DC-feed heater)	20232.5	kg/h	1	5530.2	kW	5530.2	kW	1891986.9	3280705.3
Cooler 1	17650	kg/h	1	-407.1	kW	-407.1	kW	139888.5	242566.6
Cooler 2	17650	kg/h	1	-537.2	kW	-537.2	kW	111345.0	193072.3
Cooler 3	17650	kg/h	1	-547.2	kW	-547.2	kW	113787.9	197308.3
Cooler 6	2702.39	kg/h	1	-2458.4	kW	-2458.4	kW	152874.4	265084.2
Cooler 7	31943.3	kg/h	1	-9373.8	kW	-9373.8	kW	421851.1	731489.8

Cooler 8	22014.3	kg/h	1	-4789.7	kW	-4789.7	kW	387650.4	672185.9
Cooler 9	32350.6	kg/h	1	-1990.5	kW	-1990.5	kW	155703.0	269989.1
Cooler 10	642	kmol /h	1	-11427.1	kW	-11427.1	kW	264862.3	459271.3

Component	Mass flow in	Unit	Number of equipment	Energy Consumption	Unit	Size	Unit	Equipment Cost ($)	Total installed fixed cost ($)
FEHE 7	31943.1	kg/h	1	5453.8	kW	117.4	m2	110293.9	191249.5
FEHE 8	22014.3	kg/h	1	7000.3	kW	132.1	m2	116469.8	201958.6
FEHE 9	15888.9	kg/h	1	6079.1	kW	119.0	m2	110994.1	192463.7
Hydrogen storage tank	TBC	TBC	TBC	TBC	TBC	TBC	kgH2	330 [1]	US$/kgH2
Cooling water	-43518	kW		-43518.5	kW	-0.04	GJ	0.2	$/GJ
Unit capex of CO2 storage	TBC	TBC	TBC	TBC	TBC	TBC	TBC	3450.0	€/t
DC reboiler	620.9	kg/h	1	7000.0	kW	7000.0	kW	188746.6	327286.5
DC reflux pump	640.1	kmol /h	1	11.1	kWh	11.1	kWh	55286.8	95867.3
DC-drum overhead	400.8	kmol /h	1	-	-	-		131145.4	227406.2

Section S4: Electrolyser, hydrogen storage and battery sizing

This section details the electrolyser and battery sizing method. In this scenario, the battery storage is sized big enough to sustain continuous operation during peak hours when the electricity is expensive. The battery should only provide 5 hours per week (corresponding to peak hours according to reference [23]) to avoid peak-priced electricity. The 5 hours per week is calculated from the industrial time of use tariff structure from the considered Durban (eThekwini) Municipality. The total energy demand of the system is around 126 MWh. The battery is modelled with 90% round-trip efficiency. In this paper, the Tesla Megapack Li-ion battery with a round-trip efficiency of 90 % and a power/energy ratio of 741.2 kW / 2964.8 kWh was utilised. Thus, one battery can supply 2984.8 kWh as the energy stored and 741.2 kW as the power produced, and a total of 43 batteries are required to make one modular pack. This takes into consideration the discharge efficiency and the minimum state of charge, taken as equal to 10 % of the stored electricity. Equations 7 and 8 were used for the sizing of the battery storage technology [24].

$$E_B = \frac{H \times (W_{Electrolyser} + W_{methanol\ synthesis}) \times SOC}{\eta_{RT}} \quad (7)$$

$$Number\ of\ battery\ bank = \frac{E_B}{C_B \times DOD} \quad (8)$$

The sizing of the SOEC electrolyser considered the hydrogen requirements of 2444.0 kg/h to produce 100kt/annum of methanol synthesis. The SOEC is operating under steam electrolysis. The efficiency of the electrolyser is considered 55 kWh/kg.H_2. The resultant SOEC size is about 134 MW.

The hydrogen storage tank is sized for 2hr and consequently, with an overall capacity of 4888 kg, is considered. Table S6 shows the economic assumptions related to the hydrogen storage.

Table S6: Economic assumptions related to the hydrogen storage [3].

Parameter	Value
Compressor CAPEX [€]	125 000
Tank CAPEX [€/kg H2]	300
Installation & design [% of CAPEX]	30
OPEX per year [% of CAPEX]	6.2

References

[1] Mbatha S, Cui X, Panah PG, Thomas S, Parkhomenko K, Roger AC, Louis B, Everson R, Debiagi P, Musyoka N, Langmi H. Comparative evaluation of the power-to-methanol process configurations and assessment of process flexibility. Energy Advances. 2024;3(9):2245-70.

[2] Schmidt O, Gambhir A, Staffell I, Hawkes A, Nelson J, Few S. Future cost and performance of water electrolysis: An expert elicitation study. International journal of hydrogen energy. 2017 Dec 28;42(52):30470-92.

[3] Panah PG, Cui X, Bornapour M, Hooshmand RA, Guerrero JM. Marketability analysis of green hydrogen production in Denmark: Scale-up effects on grid-connected electrolysis. International Journal of Hydrogen Energy. 2022 Mar 22;47(25):12443-55.

[4] Nemitallah MA, Alnazha AA, Ahmed U, El-Adawy M, Habib MA. Review on techno-economics of hydrogen production using current and emerging processes: Status and perspectives. Results in Engineering. 2024 Feb 8:101890.

[5] Bussche KV, Froment GF. A steady-state kinetic model for methanol synthesis and the water gas shift reaction on a commercial Cu/ZnO/Al2O3Catalyst. Journal of Catalysis. 1996 Jun 1;161(1):1-0.

[6] Van-Dal, É.S. and Bouallou, C., 2013. Design and simulation of a methanol production plant from CO2 hydrogenation. Journal of Cleaner Production, 57, pp.38-45.

[7] Mignard D, Pritchard C. On the use of electrolytic hydrogen from variable renewable energies for the enhanced conversion of biomass to fuels. Chemical engineering research and design. 2008 May 1;86(5):473-87.

[8] Cui X, Kær SK. A comparative study on three reactor types for methanol synthesis from syngas and CO2. Chemical Engineering Journal. 2020 Aug 1;393:124632.

[9] Rahimpour MR, Ghader S, Baniadam M, Fathi Kalajahi J. Incorporation of flexibility in the design of a methanol synthesis loop in the presence of catalyst deactivation. Chemical Engineering & Technology: Industrial Chemistry-Plant Equipment-Process Engineering-Biotechnology. 2003 Jun 4;26(6):672-8.

[10] Cui X, Kær SK, Nielsen MP. Energy analysis and surrogate modeling for the green methanol production under dynamic operating conditions. Fuel. 2021 Sep.

[11] Hankin A, Shah N. Process exploration and assessment for the production of methanol and dimethyl ether from carbon dioxide and water. Sustainable Energy & Fuels. 2017;1(7):1541-56.

[12] Gogate MR. Methanol synthesis revisited: reaction mechanisms in CO/CO2 hydrogenation over Cu/ZnO and DFT analysis. Petroleum Science and Technology. 2019 Mar 4;37(5):603-10.

[13] Bowker M. Methanol synthesis from CO2 hydrogenation. ChemCatChem. 2019 Sep 5;11(17):4238.

[14] Stefansson B. Power and CO2 emissions to methanol. InPresentation, 2015 European methanol policy forum 2015 Oct.

[15] Lee HW, Kim K, An J, Na J, Kim H, Lee H, Lee U. Toward the practical application of direct CO2 hydrogenation technology for methanol production. International Journal of Energy Research. 2020 Sep;44(11):8781-98.

[16] Jiang X, Nie X, Guo X, Song C, Chen JG. Recent Advances in Carbon Dioxide Hydrogenation to Methanol via Heterogeneous Catalysis. Chemical Reviews. 2020 Feb 12.

[17] Ruland H, Song H, Laudenschleger D, Stürmer S, Schmidt S, He J, Kähler K, Muhler M, Schlögl R. CO2 hydrogenation with Cu/ZnO/Al2O3: A benchmark study. ChemCatChem. 2020 Apr 21.

[18] Nestler F, Schütze AR, Ouda M, Hadrich MJ, Schaadt A, Bajohr S, Kolb T. Kinetic modelling of methanol synthesis over commercial catalysts: A critical assessment. Chemical Engineering Journal. 2020 Aug 15;394:124881.

[19] Slotboom Y, Bos MJ, Pieper J, Vrieswijk V, Likozar B, Kersten SR, Brilman DW. Critical assessment of steady-state kinetic models for the synthesis of methanol over an industrial Cu/ZnO/Al2O3 catalyst. Chemical engineering journal. 2020 Jun 1;389:124181.

[20] Lacerda de Oliveira Campos B, Herrera Delgado K, Pitter S, Sauer J. Development of consistent kinetic models derived from a microkinetic model of the methanol synthesis. Industrial & Engineering Chemistry Research. 2021 Oct 18;60(42):15074-86.

[21] G. H. Graaf, P. J. J. M. Sijtsema, E. J. Stamhuis and G. E. H. Joosten. Chemical equilibria in methanol synthesis. Chem. Eng. Sci. 41(1986) 2883–2890.

[22] Leonie E. Lücking. Methanol Production from Syngas Process modelling and design utilising biomass gasification and integrating hydrogen supply, Master Thesis (2017), Delft University of Technology.

[23] Ethekwini Municipality: https://www.durban.gov.za/storage/Documents/Service%20Tariffs/Electricity%20Tariffs/Tariffs%2023%20-%202024/Tariff%20Rates.pdf

[24] Perna A, Jannelli E, Di Micco S, Romano F, Minutillo M. Designing, sizing and economic feasibility of a green hydrogen supply chain for maritime transportation. Energy Conversion and Management. 2023 Feb 15;278:116702.